JACS
JOURNAL OF THE AMERICAN CHEMICAL SOCIETY

Communication

pubs.acs.org/JACS

Ultrafast Photoinduced Symmetry-Breaking Charge Separation and Electron Sharing in Perylenediimide Molecular Triangles

Yilei Wu,[†,§] Ryan M. Young,[†,§] Marco Frasconi,[†] Severin T. Schneebeli,[†] Peter Spenst,[‡] Daniel M. Gardner,[†,§] Kristen E. Brown,[†,§] Frank Würthner,*[,‡] J. Fraser Stoddart,*[,†] and Michael R. Wasielewski*[,†,§]

[†]Department of Chemistry and [§]Argonne–Northwestern Solar Energy Research Center, Northwestern University, 2145 Sheridan Road, Evanston, Illinois 60208-3113, United States

[‡]Institut für Organische Chemie and Center for Nanosystems Chemistry, Universität Würzburg, Am Hubland, 97074 Würzburg, Germany

Supporting Information

ABSTRACT: We report on a visible-light-absorbing chiral molecular triangle composed of three covalently linked 1,6,7,12-tetra(phenoxy)perylene-3,4:9,10-bis-(dicarboximide) (PDI) units. The rigid triangular architecture reduces the electronic coupling between the PDIs, so ultrafast symmetry-breaking charge separation is kinetically favored over intramolecular excimer formation, as revealed by femtosecond transient absorption spectroscopy. Photoexcitation of the PDI triangle dissolved in CH_2Cl_2 gives $PDI^{+\bullet}$–$PDI^{-\bullet}$ in τ_{CS} = 12.0 ± 0.2 ps. Fast subsequent intramolecular electron/hole hopping can equilibrate the six possible energetically degenerate ion-pair states, as suggested by electron paramagnetic resonance/electron–nuclear double resonance spectroscopy, which shows that one-electron reduction of the PDI triangle results in complete electron sharing among the three PDIs. Charge recombination of $PDI^{+\bullet}$–$PDI^{-\bullet}$ to the ground state occurs in τ_{CR} = 1.12 ± 0.01 ns with no evidence of triplet excited state formation.

The spatial arrangement of chromophores in multichromophoric systems governs their electronic interaction and plays an important role in both photosynthetic light harvesting and organic electronics.[1] For example, π stacking of the bacteriochlorophyll special pair comprising the primary electron donor within bacterial photosynthetic reaction center proteins results in charge-transfer character in its photoexcited singlet state, an observation that has been implicated in the overall charge separation process.[2] Photoinduced symmetry-breaking charge separation (SB-CS)[3] between two identical chromophores in nonbiological molecular assemblies is relatively uncommon because the free energy of charge separation, ΔG_{CS},[4] is rarely negative.

Irradiation of cofacial arene dimers usually leads to photodimerization or ultrafast formation of a lower-energy excimer state, which traps the excitation energy and ultimately releases it through unproductive radiative and/or nonradiative decay.[5] Neither dimerization nor excimer formation are desirable processes if the ultimate purpose is to generate charge-separated states, which are fundamental to the production of renewable solar electricity using molecular photovoltaics and stored fuels by artificial photosynthesis. In order to prevent excimer formation, we have designed and synthesized a triangle-shaped cyclic trimer containing visible-light-absorbing, redox-active 1,6,7,12-tetra(phenoxy)perylene-3,4:9,10-bis(dicarboximide) (PDI)[6] molecules. The orientation of the PDI units in a rigid triangular architecture is designed to decrease the excimer formation rate by reducing the π-orbital overlap between PDIs while still allowing some direct electronic interaction between adjacent PDI π systems.

In this work, we used fluorescence and femtosecond transient absorption (fsTA) spectroscopy to show that a compact and well-defined cyclic PDI trimer, which limits the π interaction of the PDI units, makes SB-CS between two adjacent PDI units competitive with excimer formation upon photoexcitation with visible light. Depending on the relative rates of electron transfer (ET) and hole transfer (HT), up to four energetically degenerate symmetry-broken states can be generated from the initial singlet locally excited state (S_1) (Scheme 1). Subsequent charge shifts may result in six energetically degenerate ion-pair states within the triangle. Electron

Scheme 1. Schematic of Symmetry-Breaking Charge Separation within (−)-PDI-Δ upon Photoexcitation, Showing Four Possible Charge (Hole or Electron) Transfer Processes and the Subsequent Charge Hopping between Adjacent Redox Centers To Achieve Six Energetically Degenerate Ion-Pair States

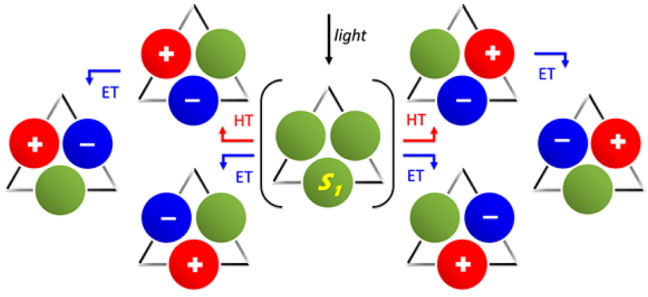

Received: August 8, 2015
Published: September 29, 2015

DOI: 10.1021/jacs.5b08386
J. Am. Chem. Soc. 2015, 137, 13236–13239

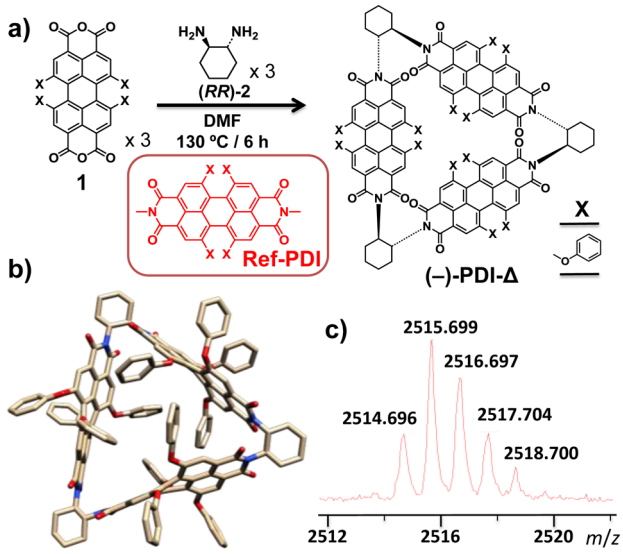

Figure 1. (a) Stereospecific synthesis of the molecular triangle (−)-**PDI-Δ** by condensation of dianhydride **1** with (*R*,*R*)-**2**. (b) Graphical representation of the DFT (B3LYP/6-31G**)-calculated structure. (c) MALDI-TOF mass spectrum of (−)-**PDI-Δ**. Calculated peaks: *m*/*z* 2514.695 (57.1%), 2515.698 (100%), 2516.701 (87.1%), 2517.705 (51.1%), 2518.708 (21.7%), 2519.711, (7.4%).

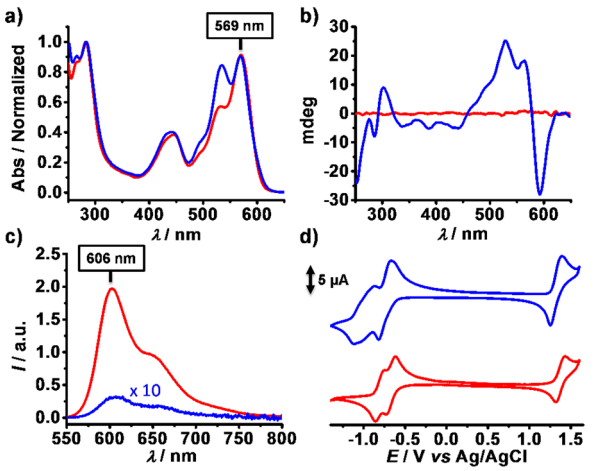

Figure 2. (a) Normalized steady-state UV−vis absorption spectra of monomeric **Ref-PDI** (red) and (−)-**PDI-Δ** (blue) in CH_2Cl_2. (b) CD spectra of Ref-PDI (red) and (−)-**PDI-Δ** (blue) in CH_2Cl_2 at 298 K and a concentration of 6 μM. (c) Steady-state emission spectra of **Ref-PDI** (red) and (−)-**PDI-Δ** (blue) in CH_2Cl_2 at 298 K (the absorbance at λ_{ex} = 535 nm was 0.102 for both samples). (d) Cyclic voltammograms of **Ref-PDI** (red) and (−)-**PDI-Δ** (blue) recorded at a scan rate of 100 mV s^{-1} using a glassy carbon working electrode. All of the experiments were performed at 298 K in Ar-purged CH_2Cl_2 solution (0.5 mM) with 0.1 M $[Bu_4N][PF_6]$ as the supporting electrolyte.

paramagnetic resonance (EPR) and electron−nuclear double resonance (ENDOR) spectroscopies show that upon mono-reduction of the cyclic trimer, the unpaired electron is shared fully among the three PDI units. These results demonstrate that good electronic communication exists between the three redox centers within the triangle architecture.

The homochiral molecular triangle, (−)-**PDI-Δ**, was prepared by a one-pot condensation[7] of (*R*,*R*)-*trans*-1,2-cyclohexanediamine ((*R*,*R*)-**2**) with 1,6,7,12-tetra(4-phenoxy)-perylene-3,4:9,10-tetracarboxylic dianhydride (**1**)[8] in *N*,*N*-dimethylformamide (DMF) at 130 °C (Figure 1a; see the Supporting Information for details). Matrix-assisted laser desorption ionization time of flight (MALDI-TOF) mass spectrometry and ^{1}H NMR spectroscopy confirmed the structure of (−)-**PDI-Δ** (Figures S1−S5). The MALDI-TOF mass spectrum of (−)-**PDI-Δ** (Figure 1c) shows the most abundant peak at *m*/*z* 2515.699, assigned to monoionized [(−)-**PDI-Δ**]$^{-\bullet}$. The ^{1}H NMR spectrum of (−)-**PDI-Δ** is broad at room temperature as a result of the rapid exchange process on the ^{1}H NMR time scale between diastereoisomers arising from the stereocenters on the cyclohexanediamine linkers and the helical chirality[9] of each of the core-twisted PDI units (P and M atropisomers). Variable-temperature ^{1}H NMR experiments on (−)-**PDI-Δ** showed splitting and sharpening of its proton resonances (Figure S3) as the interconversion between different diastereoisomeric configurations became slower on the NMR time scale with the decrease in temperature. The appearance of two sets of distinct signals points toward the existence of dynamic processes within this molecular triangle. In particular, one set of signals can be assigned to lower-symmetry (C_2 point group) (PPM)/(MMP) configurations, in which only two PDI subunits share the same chirality, and the second set can be assigned to the higher-symmetry (D_3 point group) (PPP)/(MMM) configurations, where all three PDIs share the same chirality (P or M).

The steady-state UV−vis absorption spectrum of (−)-**PDI-Δ** and a monomeric reference, **Ref-PDI**, in CH_2Cl_2 are shown in Figure 2a. (−)-**PDI-Δ** shows a pronounced intensity increase of the vibronic band centered at 535 nm with respect to that at 569 nm (ε_{max} = 1.2 × 10^5 M^{-1} cm^{-1}) indicative of excitonic coupling[10] between adjacent PDI chromophores. This spectral difference originates from a complex interplay of vibronic contributions to the excitonic couplings, which has also been observed in closely spaced cofacial dimers.[5] The circular dichroism (CD) spectrum (Figure 2b) of (−)-**PDI-Δ** displays intense optical activity, characterized by a prominent negative Cotton effect at long wavelengths when (*R*,*R*)-**2** is used as the linker. The fluorescence spectrum of (−)-**PDI-Δ** is very similar to that of **Ref-PDI**, implying that the emission occurs from the locally excited state of one PDI unit (Figure 2c). Noticeably, no red-shifted and long-lived excimer-like emission characteristic of cofacially stacked PDI derivatives is observed, ruling out the formation of an emissive excimer state. Notably, the fluorescence quantum yield of (−)-**PDI-Δ** (ϕ_F = 0.002) is significantly lower than that of **Ref-PDI** (ϕ_F = 1), which is consistent with a very efficient nonradiative decay process such as SB-CS.

In order to estimate the free energy changes required for SB-CS, we performed cyclic voltammetry on **Ref-PDI** and (−)-**PDI-Δ** in dry CH_2Cl_2 under argon (Figure 2d) to determine their redox potentials. These data are reported in Table S1 along with the excitation energies and estimated values of ΔG_{CS}. **Ref-PDI** exhibits two distinct reversible reduction waves and one quasi-reversible oxidation wave, like other tetraphenoxy-substituted PDIs.[6] (−)-**PDI-Δ** shows similar behavior, but the waves are cathodically shifted by ca. 50 mV and slightly broadened, which may be caused by multielectron processes.[5c] However, the difference between the first oxidation and reduction potentials remains unchanged. Thus, using the Weller treatment[4] gives $\Delta G_{CS} \approx -0.19$ eV for SB-CS within (−)-**PDI-Δ** in CH_2Cl_2.

DOI: 10.1021/jacs.5b08386
J. Am. Chem. Soc. 2015, 137, 13236−13239

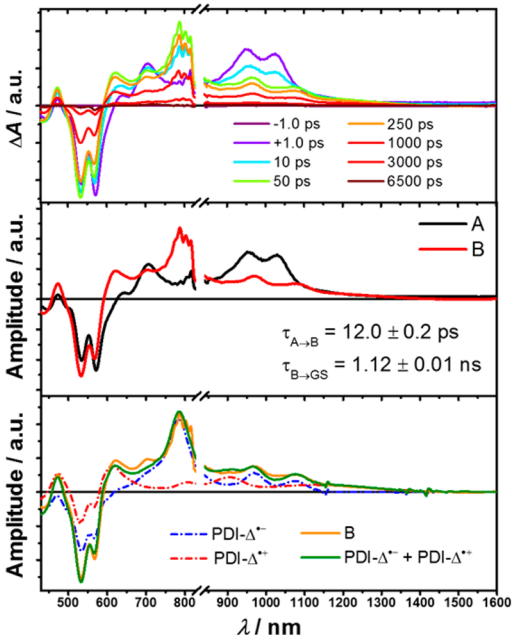

Figure 3. (top) Femtosecond transient absorption of (−)-**PDI-Δ** showing the excited-state dynamics after photoexcitation. (middle) Species-associated spectra reconstructed from global fits to the sequential A → B → ground state (GS) model, where A is ^{1}*PDI and B is the SB-CS state (λ_{ex} = 569 nm, 1.0 μJ/pulse, CH_2Cl_2, 298 K, air-equilibrated). (bottom) Comparison of the transient absorption spectrum of the B = SB-CS state with the differential static spectra of [(−)-**PDI-Δ**]$^{-\bullet}$ and [(−)-**PDI-Δ**]$^{+\bullet}$ generated by chemical reduction and oxidation, respectively, and their sum [(−)-**PDI-Δ**]$^{-\bullet}$ + [(−)-**PDI-Δ**]$^{+\bullet}$.

We carried out fsTA studies of (−)-**PDI-Δ** in CH_2Cl_2 in order to elucidate the excited-state dynamics responsible for its efficient nonradiative decay. The fsTA spectra of (−)-**PDI-Δ** are shown in Figure 3, and for comparison, those of **Ref-PDI** are given in Figure S6. The fsTA spectra of **Ref-PDI** following a 569 nm, 100 fs laser pulse feature ground-state bleaching (GB) at 450, 533, and 571 nm, stimulated emission (SE) at 600 and 650 nm, and excited singlet state (^{1}*PDI) absorption (ESA) at 709, 947, and 1028 nm.[11] On the other hand, (−)-**PDI-Δ** shows very different excited-state dynamics characterized by fast decay of the ^{1}*PDI-Δ state (ESA at 705, 951, and 1028 nm; Figure S9) in τ_{CS} = 12.0 ± 0.2 ps to give a new transient species characterized by positive features in the visible region at 473 and 619 nm and in the near-IR region at 780, 969, and 1077 nm, corresponding to the spectral features of PDI radical cation[6b,8] and PDI radical anion (vide infra), respectively. The observed ultrafast transient dynamics shows photoinduced intramolecular SB-CS behavior of (−)-**PDI-Δ**, consistent with its quenched fluorescence. The SB-CS state decays by charge recombination (CR) to the ground state in τ_{CR} = 1.12 ± 0.01 ns in CH_2Cl_2 with no evidence of triplet excited state formation. The much slower charge recombination relative to charge separation, even though the former process is quite exothermic, is consistent with the fact that the recombination lies far into the Marcus inverted region.[12] We also performed fsTA measurements in $CHCl_3$ (dielectric constant (ε_S) = 4.81, $\Delta G_{CS} \approx -0.02$ eV) and in toluene (ε_S = 2.38, $\Delta G_{CS} \approx 0.22$ eV) in order to probe the effect of solvent polarity on SB-CS. In $CHCl_3$ (Figures S12 and S13) we found that charge separation slows to τ_{CS} = 59.2 ± 0.6 ps and the SB-CS lifetime is extended to τ_{CR} = 4.36 ± 0.02 ns, in line with Marcus theory. In less polar toluene (Figures S16 and S17), the SB-CS process is switched off because the ion-pair state has a higher energy than the excited singlet state.

Given the relatively small ΔG_{CS} for SB-CS in (−)-**PDI-Δ**, modulation of ΔG_{CS} and the electronic-coupling matrix element for this process by structural fluctuations in the PDI units and/or the surrounding solvent are most likely responsible for the observed ultrafast rate. We do in fact observe a relaxation process in ^{1}*[**Ref-PDI**] that occurs with $\tau \approx 75$ ps (Figures S6 and S7). This relaxation can be related to a twisting of the PDI core or even to movement of the phenoxy rings upon photoexcitation.[13] Structural changes of a similar type in (−)-**PDI-Δ** may be enough to break the symmetry and induce charge separation, although we do not directly observe such features in the transient absorption data for (−)-**PDI-Δ** (Figure S8).

Redox titration experiments were performed in order to confirm the electronic absorption features of the charge-separated state. Upon addition of 1 equiv of cobaltocene ($CoCp_2$) (E = −1.0 V vs SCE, CH_2Cl_2), the decrease in the neutral-state absorption band is accompanied by the appearance of new bands at 783, 970, and 1078 nm (Figure S19). On the other hand, partial oxidation of (−)-**PDI-Δ** with $NOPF_6$ (E = 1.46 V vs SCE, CH_2Cl_2) results in the appearance of positive features at 474, 613, 805, 908, and 1142 nm (Figure S20).

Femtosecond stimulated Raman spectroscopy (FSRS) further corroborates our interpretation of the fsTA results (Figures S21 and S22). The FSRS spectrum of **Ref-PDI** is characterized by monoexponential decay of vibrational modes between 1000 and 1600 cm^{-1}. The same vibrations in (−)-**PDI-Δ** are observed to decay in τ_{CS} = 11.5 ± 0.6 ps, giving rise to new vibrational features that overlay with (−)-**PDI-Δ** anion modes generated by chemical oxidation. The recombination time, τ_{CR} = 1.0 ± 0.1 ns, is consistent with that observed by fsTA within experimental error.

Because of the ease of generating monoreduced states of **Ref-PDI** and (−)-**PDI-Δ**, we performed EPR and ENDOR spectroscopy to probe electron sharing among adjacent PDI units within (−)-**PDI-Δ**. Continuous-wave (CW) EPR measurements at room temperature show that the spectrum of [(−)-**PDI-Δ**]$^{-\bullet}$ is narrowed compared with that of [**Ref-PDI**]$^{-\bullet}$ (Figure 4a). The spectral narrowing and subsequent loss of hyperfine structure are indicative of efficient electron sharing over multiple PDI units, as seen previously in very large cofacial PDI aggregates and PDI-containing DNA hairpins.[14] Additionally, the ENDOR spectrum of [(−)-**PDI-Δ**]$^{-\bullet}$ (Figure

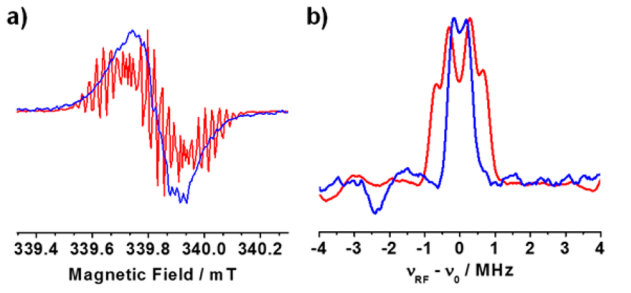

Figure 4. (a) CW EPR and (b) ^{1}H ENDOR spectra of [**Ref-PDI**]$^{\bullet-}$ (red) and [(−)-**PDI-Δ**]$^{\bullet-}$ (blue) produced by monoreduction of **Ref-PDI** and (−)-**PDI-Δ**, respectively, with 1 equiv of $CoCp_2$ in CH_2Cl_2 at 298 K.

DOI: 10.1021/jacs.5b08386
J. Am. Chem. Soc. 2015, 137, 13236−13239

4b) shows a clear reduction in the isotropic hyperfine coupling constant (a_H) by a factor of 3 compared with that of [**Ref-PDI**]$^{-\bullet}$, meaning that the unpaired electron is shared[14c] among all three PDIs within the molecular triangle at a rate exceeding that measurable on the ENDOR time scale (>10^7 s^{-1}). Remarkably, [(−)-**PDI-Δ**]$^{-\bullet}$ gives a CW EPR signal that is narrowed with respect to the PDI reference even at 85 K (Figure S23), which indicates that complete electron sharing continues at lower temperatures.

In summary, we have synthesized a visible-light-harvesting molecular triangle that can undergo ultrafast photoinduced intramolecular symmetry-breaking charge separation in a manner similar to the primary electron donor in bacterial photosynthetic reaction center proteins. We have demonstrated that the rigid molecular triangle architecture can effectively slow down excimer formation, which kinetically outcompetes SB-CS in most π-stacked dimers of aromatic molecules. Moreover, we have shown that full electron sharing takes place among the three PDI units within the triangular geometry, implying fast electron hopping between adjacent redox centers. Our findings have potential utility in the design of new molecular materials for solar energy conversion and organic electronics.

■ ASSOCIATED CONTENT

Supporting Information

The Supporting Information is available free of charge on the ACS Publications website at DOI: 10.1021/jacs.5b08386.

Experimental details, including synthesis, NMR, fsTA, FSRS, and electrochemical experiments (PDF)

■ AUTHOR INFORMATION

Corresponding Authors

*m-wasielewski@northwestern.edu
*stoddart@northwestern.edu
*wuerthner@chemie.uni-wuerzburg.de

Notes

The authors declare no competing financial interest.

■ ACKNOWLEDGMENTS

This work was supported by the Chemical Sciences, Geosciences, and Biosciences Division, Office of Basic Energy Sciences, U.S. Department of Energy under Grant DE-FG02-99ER14999. M.R.W. thanks the Alexander von Humboldt Foundation for a research award. Synthesis was supported by the National Science Foundation under CHE-1308107 (J.F.S.). This research is part of the Joint Center of Excellence in Integrated Nano-Systems at King Abdul-Aziz City for Science and Technology and Northwestern (Project 34-947). F.W. and P.S. thank the DFG for financial support of their project Wu 317/15 within the collaborative research unit FOR1809. Y.W. thanks the Fulbright Scholar Program for a fellowship and the NU International Institute of Nanotechnology for a Ryan Fellowship.

■ REFERENCES

(1) (a) Gust, D.; Moore, T. A.; Moore, A. L. *Acc. Chem. Res.* **2001**, *34*, 40. (b) Holten, D.; Bocian, D. F.; Lindsey, J. S. *Acc. Chem. Res.* **2002**, *35*, 57. (c) Ferreira, K. N.; Iverson, T. M.; Maghlaoui, K.; Barber, J.; Iwata, S. *Science* **2004**, *303*, 1831. (d) Guldi, D. M. *J. Phys. Chem. B* **2005**, *109*, 11432. (e) Wasielewski, M. R. *Acc. Chem. Res.* **2009**, *42*, 1910. (f) Aratani, N.; Kim, D.; Osuka, A. *Acc. Chem. Res.* **2009**, *42*, 1922. (g) Weil, T.; Vosch, T.; Hofkens, J.; Peneva, K.; Müllen, K. *Angew. Chem., Int. Ed.* **2010**, *49*, 9068. (h) Bhosale, R.; Misek, J.; Sakai, N.; Matile, S. *Chem. Soc. Rev.* **2010**, *39*, 138. (i) Saeki, A.; Koizumi, Y.; Aida, T.; Seki, S. *Acc. Chem. Res.* **2012**, *45*, 1193. (j) Fukuzumi, S.; Ohkubo, K.; D'Souza, F.; Sessler, J. L. *Chem. Commun.* **2012**, *48*, 9801.

(2) (a) Won, Y.; Friesner, R. A. *Proc. Natl. Acad. Sci. U. S. A.* **1987**, *84*, 5511. (b) Lathrop, E. J. P.; Friesner, R. A. *J. Phys. Chem.* **1994**, *98*, 3056. (c) Laporte, L. L.; Palaniappan, V.; Kirmaier, C.; Davis, D. G.; Schenck, C. C.; Holten, D.; Bocian, D. F. *J. Phys. Chem.* **1996**, *100*, 17696. (d) Huang, L. B.; Ponomarenko, N.; Wiederrecht, G. P.; Tiede, D. M. P. *Proc. Natl. Acad. Sci. U. S. A.* **2012**, *109*, 4851. (e) Harris, M. A.; Luehr, C. A.; Faries, K. M.; Wander, M.; Kressel, L.; Holten, D.; Hanson, D. K.; Laible, P. D.; Kirmaier, C. *J. Phys. Chem. B* **2013**, *117*, 4028.

(3) For reviews on SB-CS, see: (a) Grabowski, Z. R.; Rotkiewicz, K.; Rettig, W. *Chem. Rev.* **2003**, *103*, 3899. (b) Vauthey, E. *ChemPhysChem* **2012**, *13*, 2001. For research articles, see: (c) Schneider, F.; Lippert, E. *Ber. Bunsen-Ges.* **1968**, *72*, 1155. (d) Piet, J. J.; Schuddeboom, W.; Wegewijs, B. R.; Grozema, F. C.; Warman, J. M. *J. Am. Chem. Soc.* **2001**, *123*, 5337. (e) Mataga, N.; Yao, H.; Okada, T.; Rettig, W. *J. Phys. Chem.* **1989**, *93*, 3383. (f) Giaimo, J. M.; Gusev, A. V.; Wasielewski, M. R. *J. Am. Chem. Soc.* **2002**, *124*, 8530. (g) Holman, M. W.; Yan, P.; Adams, D. M.; Westenhoff, S.; Silva, C. *J. Phys. Chem. A* **2005**, *109*, 8548. (h) Markovic, V.; Villamaina, D.; Barabanov, I.; Lawson Daku, L. M.; Vauthey, E. *Angew. Chem., Int. Ed.* **2011**, *50*, 7596. (i) Whited, M. T.; Patel, N. M.; Roberts, S. T.; Allen, K.; Djurovich, P. I.; Bradforth, S. E.; Thompson, M. E. *Chem. Commun.* **2012**, *48*, 284.

(4) Weller, A. *Z. Phys. Chem.* **1982**, *133*, 93.

(5) (a) Staab, H. A.; Riegler, N.; Diederich, F.; Krieger, C.; Schweitzer, D. *Chem. Ber.* **1984**, *117*, 246. (b) Fink, R. F.; Seibt, J.; Engel, V.; Renz, M.; Kaupp, M.; Lochbrunner, S.; Zhao, H. M.; Pfister, J.; Würthner, F.; Engels, B. *J. Am. Chem. Soc.* **2008**, *130*, 12858. (c) Schlosser, F.; Moos, M.; Lambert, C.; Würthner, F. *Adv. Mater.* **2013**, *25*, 410. (d) Brown, K. E.; Salamant, W. A.; Shoer, L. E.; Young, R. M.; Wasielewski, M. R. *J. Phys. Chem. Lett.* **2014**, *5*, 2588. (e) Wu, Y. L.; Frasconi, M.; Gardner, D. M.; McGonigal, P. R.; Schneebeli, S. T.; Wasielewski, M. R.; Stoddart, J. F. *Angew. Chem., Int. Ed.* **2014**, *53*, 9476. (f) Lindquist, R. J.; Lefler, K. M.; Brown, K. E.; Dyar, S. M.; Margulies, E. A.; Young, R. M.; Wasielewski, M. R. *J. Am. Chem. Soc.* **2014**, *136*, 14912. (g) Son, M.; Fimmel, B.; Dehm, V.; Würthner, F.; Kim, D. *ChemPhysChem* **2015**, *16*, 1757.

(6) For example, see: (a) Langhals, H. *Heterocycles* **1995**, *40*, 477. (b) Kircher, T.; Lohmannsroben, H. G. *Phys. Chem. Chem. Phys.* **1999**, *1*, 3987. (c) Gvishi, R.; Reisfeld, R.; Burshtein, Z. *Chem. Phys. Lett.* **1993**, *213*, 338. (d) Würthner, F. *Chem. Commun.* **2004**, 1564.

(7) Schneebeli, S. T.; Frasconi, M.; Liu, Z.; Wu, Y.; Gardner, D. M.; Strutt, N. L.; Cheng, C.; Carmieli, R.; Wasielewski, M. R.; Stoddart, J. F. *Angew. Chem., Int. Ed.* **2013**, *52*, 13100.

(8) Würthner, F.; Sautter, A.; Schmid, D.; Weber, P. J. A. *Chem. - Eur. J.* **2001**, *7*, 894.

(9) Osswald, P.; Würthner, F. *J. Am. Chem. Soc.* **2007**, *129*, 14319.

(10) Kasha, M.; Rawls, H. R.; El-Bayoumi, M. A. *Pure Appl. Chem.* **1965**, *11*, 371.

(11) These features occur within the instrument response function and decay with τ = 6.6 ± 0.1 ns in CH_2Cl_2, in agreement with the reported singlet lifetime (see ref 6c) within instrumental error.

(12) Marcus, R. A.; Sutin, N. *Biochim. Biophys. Acta, Rev. Bioenerg.* **1985**, *811*, 265.

(13) Fron, E.; Schweitzer, G.; Osswald, P.; Würthner, F.; Marsal, P.; Beljonne, D.; Müllen, K.; De Schryver, F. C.; Van der Auweraer, M. *Photochem. Photobiol. Sci.* **2008**, *7*, 1509.

(14) (a) Che, Y. K.; Datar, A.; Yang, X. M.; Naddo, T.; Zhao, J. C.; Zang, L. *J. Am. Chem. Soc.* **2007**, *129*, 6354. (b) Chen, S. G.; Branz, H. M.; Eaton, S. S.; Taylor, P. C.; Cormier, R. A.; Gregg, B. A. *J. Phys. Chem. B* **2004**, *108*, 17329. (c) Wilson, T. M.; Zeidan, T. A.; Hariharan, M.; Lewis, F. D.; Wasielewski, M. R. *Angew. Chem., Int. Ed.* **2010**, *49*, 2385.

DOI: 10.1021/jacs.5b08386
J. Am. Chem. Soc. 2015, 137, 13236−13239